Asymmetric rostro-caudal inhibition in the primary olfactory cortex

Victor M. Luna and **Diana L. Pettit**[*]

Department of Neuroscience, Albert Einstein College of Medicine

Abstract

The importance of intracortical inhibitory circuits in setting the feature-selective spatial organization of primary sensory cortices remains controversial. To address this issue, we examined the strength of interneuron-to-pyramidal cell connections across the rat anterior piriform cortex (aPC) and found a pronounced gradient of increasing pyramidal cell inhibition along the aPC rostro-caudal axis. This functional heterogeneity could govern aPC spatial activation in response to varying odor identities and features.

Precise timing of inhibition has been proposed to be a key mechanism in primary sensory cortices for tuning pyramidal cell spike output to sensory-evoked inputs[1,2,3,4,5]. Whether local inhibitory circuits are also involved in establishing the feature-selective spatial organization of primary sensory cortices has been the subject of considerable debate[6]. At the crux of the controversy is the issue of how local inhibitory circuits are organized across cortical space. In order to test this idea, we examined the strength of inhibitory connections onto pyramidal cells along the aPC rostro-caudal axis.

To date, all studies that have investigated the intracortical connective organization of the aPC have been anatomical in nature and as such have not characterized functional synapses[7]. To assess functional interneuron-to-pyramidal cell connections, we uncaged glutamate focally over Layer 1, 2, or 3 interneurons and recorded the resulting $GABA_A$ receptor-mediated inhibitory postsynaptic currents (IPSCs) in Layer 2/3 pyramidal cells[4] (Fig. 1a and Supplementary methods; see Supplementary Fig. 1 for uncaging beam spatial resolution). We then used IPSC charge as our measure for strength of connectivity (Fig. 1a). This approach allowed us to sample a large, spatially distributed pool of layer-specific inhibitory connections onto a single pyramidal cell (Fig. 1a,b).

We found that the location of an interneuron relative to a pyramidal cell dictates connective strength. Pyramidal cell IPSC charge gradually increased as we moved our uncaging beam from rostral to caudal locations relative to the cell soma (Fig. 1a,b and Supplementary Fig. 2). When we compared caudal uncaging spots (positions 50 to 450 μm in Fig. 1b) with their

[*]Correspondence should be addressed to D.L.P. (diana.pettit@einstein.yu.edu).

Author contributions

V.M.L performed and analyzed experiments. V.M.L and D.L.P. designed the experiments and prepared the manuscript.

equidistant rostral counterparts (positions −50 to −450 μm in Fig. 1b), we found that IPSC charge evoked by caudal uncaging spots were significantly larger than those elicited by rostral spots (Fig. 1c). On average, the caudal/rostral ratio of IPSC charge (Fig. 1c) was 1.6±0.2 for Layer 1 (mean±s.e.m.; P=0.002; n=26), 1.8±0.2 for Layer 2 (P=0.0001), and 2.0±0.1 for Layer 3 (P=0.0002).

To determine whether inhibitory asymmetry is unique to pyramidal cells, we compared inhibitory connections onto Layer 2 bitufted interneurons and adjacent pyramidal cells (< 150 μm apart) in the same slice (Fig. 1d,e). We selected bitufted interneurons because, like pyramidal cells, their dendrites project across all aPC layers. We identified bitufted interneurons based on their distinct bipolar apical and basal dendrites[8] and depolarized resting membrane potentials (−51±4 vs. −60±2 mV; Fig. 1d and Supplementary methods). In stark contrast to their adjacent pyramidal cells, we found that inhibition onto bitufted interneurons was highly symmetric in all aPC layers (Fig. 1d,e and Supplementary Fig. 2). This indicates that asymmetric rostro-caudal inhibition is a distinct pyramidal cell-specific mechanism. Further, it suggests that the differential inhibition is not an artifact of the brain slicing procedure.

Since inhibition of a pyramidal cell increases along the aPC rostro-caudal axis (Fig. 1), we hypothesized that pyramidal cells located caudally should receive greater inhibition than those located rostrally. We tested this possibility by comparing inhibitory inputs to pairs of pyramidal cells in the same slice (Fig. 2a). We found significant differences in inhibition across all aPC layers for cells separated by at least 200 μm (Fig. 2b). Layer 1 interneurons evoked a mean charge of 2.9±1.0 pA.sec in caudal versus 1.4±0.6 pA.sec in rostral pyramidal cells (P=0.02; n=8 cell pairs). Layer 2 interneurons evoked a mean charge of 9.6±2.5 pA.sec in caudal versus 4.9±1.6 in rostral cells (P=0.0001; n=8). Layer 3 interneurons evoked a mean charge of 6.2±1.5 pA.sec in caudal versus 2.2±0.8 in rostral cells (P=0.0001; n=8). Thus, the strength of inhibition onto pyramidal cells occurs as a gradient, increasing in magnitude along rostal-caudal space. Further, differences in inhibitory input strength over relatively short distances (~200 μm) suggest that local circuits differ widely within the aPC. Due to this functional spatial heterogeneity, discrete computational units—analogous to barrels and columns in other sensory cortices—could potentially be formed on the basis of significant differences in rostro-caudal inhibition.

Because pyramidal cells located at more caudal aPC regions receive greater inhibition than cells at rostral locations, caudal pyramidal cells should require greater olfactory bulb excitation than rostral cells to spike. Consequently, increases in olfactory bulb activity, as seen with increased odor concentration[9], would be represented as a gradual recruitment of pyramidal cell spike activity from rostral to caudal aPC locations. Indeed, *in vivo* unit recordings have shown a spatial gradient of increasing spike activity from rostral to caudal aPC regions with increasing odor concentrations[10]. Thus, the asymmetric nature of pyramidal cell inhibition could be a fundamental organizational principle that governs how the aPC represents changes in odor features at both the single cell and population level.

Experiments focused on determining the mechanisms underlying differential rostro-caudal inhibition should lead to an even better understanding of its computational significance. Our

findings provide a couple of important insights into the properties of these mechanisms. First, there must be a target cell-specific mechanism that restricts asymmetric inhibition to pyramidal cells (Fig. 1). Second, there must be a mechanism that allows pyramidal cell inhibition to differ greatly over short distances (~200 μm; Fig. 2). Increasing interneuron cell density along the aPC rostro-caudal axis is perhaps the simplest mechanism that could account for asymmetric inhibition. However, because of target cell-specificity (Fig. 1d,e and Supplementary Fig. 2) and because asymmetric inhibition occurs over narrow cortical areas (Fig. 2), it is unlikely that increased interneuron cell density underlies the differential inhibition of pyramidal cells. In fact, thorough anatomical studies indicate that any appreciable difference in interneuron density could only be observed along rostro-caudal distances of ~2000 μm[11], an order of magnitude larger than our rostral-caudal gradient threshold of 200 μm (Fig. 2). More plausible mechanisms include, but are not restricted to: (1) marked differences in intrinsic interneuron excitability that allow caudal interneurons to fire more action potentials than rostral interneurons, (2) differences in interneuron presynaptic release machinery that allow caudal interneurons to release more GABA than rostral interneurons, and (3) skewed interneuron axon projections that make it possible for caudal interneurons to more robustly inhibit pyramidal cells. Further, multiple cellular and circuit mechanisms working independently or in concert may be in play for differential pyramidal cell inhibition to arise.

Supplementary Material

Refer to Web version on PubMed Central for supplementary material.

Acknowledgments

References

1. Hirsch JA, Alonso JM, Reid RC, Martinez LM. J Neurosci. 1998; 18:9517–9528. [PubMed: 9801388]

2. Wehr M, Zador AM. Nature. 2003; 426:442–446. [PubMed: 14647382]

3. Wilent WB, Contreras D. Nat Neurosci. 2005; 8:1364–1370. [PubMed: 16158064]

4. Luna VM, Schoppa NE. J Neurosci. 2008; 28:8851–8859. [PubMed: 18753387]

5. Poo C, Isaacson JS. Neuron. 2009; 62:850–861. [PubMed: 19555653]

6. Priebe NJ, Ferster D. Neuron. 2008; 57:482–497. [PubMed: 18304479]

7. Neville, KR.; Haberly, LB. The synaptic organization of the brain. 5. Shepherd, GM., editor. Oxford Univ. Press; New York: 2004. p. 415-454.

8. Ekstrand JJ, Domroese ME, Feig SL, Illig KR, Haberly LB. J Comp Neurol. 2001; 434:308–328. [PubMed: 11331531]

9. Johnson BA, Leon M. J Comp Neurol. 2007; 503:1–34. [PubMed: 17480025]

10. Sugai T, Miyazawa T, Fukuda M, Yoshimura H, Onoda N. Neuroscience. 2005; 130:769–781. [PubMed: 15590159]

11. Löscher W, Lehmann H, Ebert U. Brain Res. 1998; 800:21–31. [PubMed: 9685574]

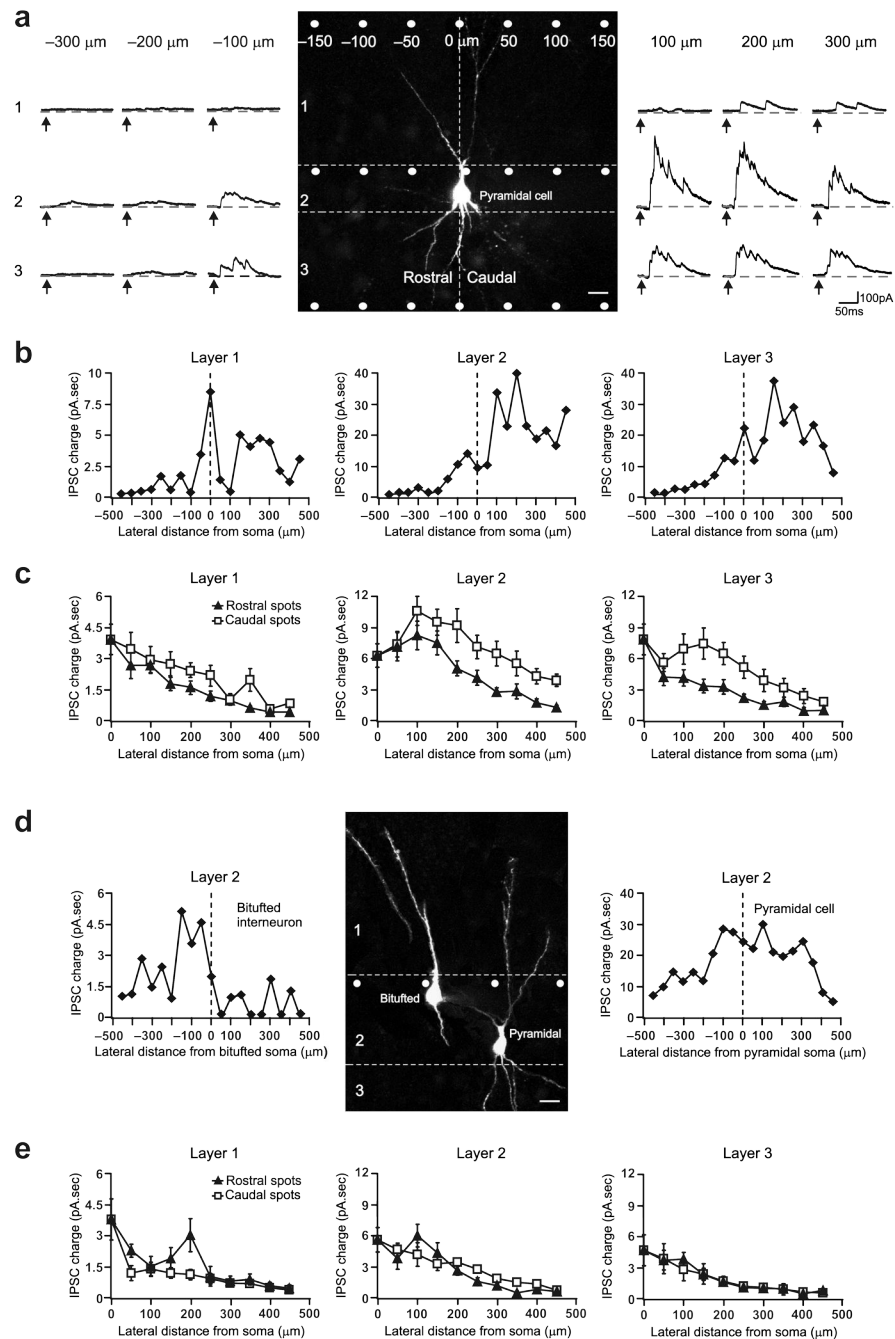**Figure 1. Asymmetric inhibition along the aPC rostro-caudal axis**

a) The uncaging beam (white spot) was pulsed at 50 μm lateral intervals from the pyramidal cell soma (V_h=0 mV). Photolysis of glutamate caused interneurons under the uncaging beam to spike, eliciting IPSCs in connected cells. *Right/Left*, Photostimulation-evoked IPSCs recorded in the representative pyramidal cell. Arrows indicate uncaging pulse onset. IPSC charge was measured as the current area above baseline (dashed lines). Note the increase in IPSC charge from rostral to caudal uncaging spots. The pyramidal cell soma was designated as position 0. 25μm scale bar. **b)** Scatter plot of uncaging spot location versus IPSC charge

showing the gradual increase in IPSC charge along the rostro-caudal axis for the cell in **(a). c)** Scatter plot of uncaging spot location versus mean IPSC charge showing that, on average, caudal spots evoked significantly larger IPSCs than equidistant rostral spots in 26 pyramidal cells. **d)** *Right/Left*, Layer 2 inhibitory input onto a bitufted interneuron and a pyramidal cell. 20 μm scale bar. **e)** Caudal and rostral uncaging spots evoked similar IPSC charge in 8 bitufted interneurons. s.e.m. bars are indicated in (c) and (e).
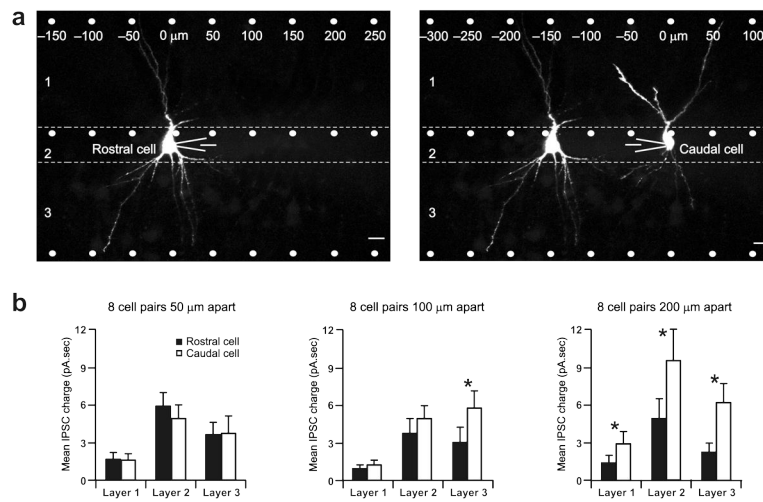
Figure 2. Caudal pyramidal cells receive stronger inhibitory input than rostral cells
a) Mapping inhibitory connections onto a rostral and caudal pyramidal cell separated by 100 μm in the same slice. 25μm scale bars. **b)** Comparison of mean IPSC charge (from uncaging spot positions −450 to 450 μm) of rostral versus caudal pyramidal cells that are 50, 100, and 200μm apart. *P<0.02. s.e.m. bars are indicated.